Energy saving and indoor thermal comfort evaluation using a novel local exhaust ventilation system for office rooms

Ahmed Qasim Ahmed*, Shian Gao, Ali Khaleel Kareem

Department of Engineering, University of Leicester, Leicester LE1 7RH, United Kingdom

*Corresponding author: phone: +44(0)116 252 2874; fax: +44(0)116 252 2525; e-mail: aqaa2@ le.ac.uk.

Abstract:

Energy saving, indoor thermal comfort and inhaled air quality in an office are strongly affected by the flow interaction in the micro-environment around the occupants. The local exhaust ventilation system, which aims to control the transmission of contaminant and extract contaminant air locally, is widely used in industrial applications. In this study, the concept of the local exhaust ventilation system is developed for use in office applications. Consequently, a novel local exhaust ventilation system for offices was combined with an office work station in one unit. Energy saving, thermal comfort and inhaled air quality were used to evaluate the performance of the new system. Experimental data from published work are used to validate the computational fluid dynamic model of this study. The performance of the new system for three different amounts of recirculated air (35%, 50%, and 65% of the total mass flow rate) was investigated numerically in an office room with and without using the new system to show its impact on energy saving, thermal comfort and inhaled air quality. The result shows that the new local exhaust ventilation system can reduce the energy consumption by up to 30%, compared with an office not using this system. Furthermore, this system was able to reduce the contaminant concentration in a micro-environment area by up to 61% and improve the human thermal comfort in the occupied zone. It can be concluded that using the local exhaust

ventilation concept can make significant improvements to the quality of inhaled air and produce extra energy saving with an acceptable thermal comfort.

Keywords: Energy saving, Thermal comfort, Displacement ventilation, Local exhaust ventilation

Nomenclature

Abbreviations

DV	Displacement Ventilation
IAQ	Indoor Air Quality
LEV	Local Exhaust Ventilation
LEVO	Local Exhaust Ventilation for Office
PMV	Predicted Mean Vote
PPD	Predicted Percentage of Dissatisfied
STRAD	Stratified Air Distribution System

Latin letters

C	mean particle concentration (kg/m^3)
$C_{1\varepsilon}$, $C_{2\varepsilon}$	model constants in the term ε of the turbulence model
C_n	normalised concentration.
C_p	contaminant concentration in a specific region (kg/m^3)
C_e	the concentration at exhaust (kg/m^3)
C_μ	model constant of the turbulence model
c_p	specific heat of air at constant pressure (J/(kg K)
d_p	particle diameter (m)
dt	particle residence time (s)
F_D	inverse of relaxation time (s^{-1})
$\vec{F}_a$	force acting on particle (m/s^2)
$\vec{F}_b$	Brownian force (m/s^2)
$\vec{F}_{thermal}$	thermophoretic force (m/s^2)
$\vec{F}_s$	Saffman's lift forces (m/s^2)
$\vec{g}$	gravitational acceleration (m/s^2)
i	trajectory index
j	cell index
k	turbulent kinetic energy per unit mass (J/kg)
$\dot{m}$	mass flow rate associated with each trajectory (kg/s)
$\dot{m}_e$	exhaust mass flow rate (kg/s)
n	trajectory number
P_k	additional term in the turbulence model
$Q_{coil-STRA}$	cooling coil load for the STRAD system (W)
Q_{space}	cooling coil load of space (W)
Q_{vent}	ventilation load (W)
$Q_{coil-MV}$	cooling coil load for the mixing ventilation system (W)
S	mean strain rate tensor magnitude
S_{ij}	strain rate tensor
T_e	the exhaust temperature (°C)
T_{set}	room set temperature (°C)
t	time (s)
$\vec{u}_p$	particle velocity vector (m/s)
u	fluid velocity (m/s)
u_i'	fluctuating velocity (m/s)
V_j	volume associated with i trajectory and cell j

Greek letters

β	coefficient of thermal expansion (1/K)
ε	turbulent dissipation rate (m^2/s^3)
λ	represents the molecular mean free path
μ	dynamic viscosity (kg/(m s)
ξ_i	normally distributed random number
ρ	fluid density (kg/m^3)
ρ_p	particle density (kg/m^3)
σ_k	model constant for k equation of the turbulence model
σ_ε	model constant for ε equation of the turbulence model

1 Introduction

Most people spend the majority of their time indoors [1-3]. Therefore, Indoor Air Quality (IAQ) and human thermal comfort should be maintained at a high level. In recent decades, various ventilation methods and devices have been developed to provide a comfortable thermal environment for occupants and to reduce the demand for energy [4-7]. In addition, one of the most important strategies is to use a Local Exhaust Ventilation (LEV) system, also called the Personalised Exhaust (PE) system. In this system, warm and contaminated air is extracted locally before reaching the occupied area, which consequently enhances the quality of the inhaled air. The LEV system is not a new method of ventilation. It is used to control the contaminant transmission in occupied areas [8-11] and has been widely used in industrial applications to provide a healthy and comfortable work space. Melikov et al. [12] used an LEV concept to develop the thermal environment around a hospital bed and investigated the reduction of the exposure for the doctor and the patient with and without the LEV system. They found that with the LEV system the exposure level was reduced significantly for people who sat close to the patient. Dygert and Dang [9] proposed to use a local exhaust suction device in an airplane, and their results showed that up to 90% reduction of exposure to contamination comes from other passengers. Furthermore, they concluded that this type of LEV is suited to a high density occupation. Zítek et al. [11] investigated the thermal environment and the air quality around the occupants in an aircraft using a separate air flow supply and a separate local exhaust. Their results showed that using this system protected the occupants from possible dispersion of disease in an aircraft environment. Qian et al. [13] considered the pollutant transmission in a hospital ward using a downward ventilation system. They found that the fine particle removal efficiency was improved by using an exhaust at a high level, while locating the exhaust at a low level improved the particle removal efficiency for large-size particles. Cheong and Phua [14] examined the performance of contaminant removal using different strategies of ventilation system in hospital rooms. They found that the best performance in contaminant removal occurred by situating the supply and exhaust diffuser on the wall behind the patient's bed. Neilsen et al. [15] studied the risk of cross-contamination in a hospital room using a downward ventilation system. They revealed that the position of the return openings played a significant role in the transmission of exhaled contaminants in the room. Yang et al. [16] researched the performance of three different kinds of personalised exhaust (PE) device. They found that the quality of the inhaled air was enhanced by using a PE just above the occupant's shoulder level. Bolashikov et al. [17] explored the thermal environment around the occupant by combining the local exhaust with a local supply using a seat-incorporated with a Personalized Ventilation (PV) unit. They found that using this system enabled them to enhance the quality of the inhaled air. Junjing et al. [18] looked into the performance of contaminant removal effectiveness at 12 different locations by using a PE-PV system installed on the chair above the occupant's shoulder level. They found that using this system enhanced the inhaled air quality for the seated persons compared with using a PV system alone.

The previous studies focused on using a LEV system in hospitals rooms, airplanes and on some industrial applications to improve the quality of the inhaled air and provide a healthy and comfortable environment for the occupants. However, very limited studies have considered the LEV as a ventilation system in an office space [16, 17], and its impact on the energy consumption. Therefore, in this study a novel ventilation system, the Local Exhaust Ventilation for Office (LEVO) system, was investigated numerically to show the effects of using this system on the energy saving and thermal environment around the occupants. In general, most indoor contaminants in an office arise from furniture, work station equipment and by occupants' activities and may contain chemical substances [19, 20]. Therefore, in this study the contaminants were released from two pollutant sources: one is located at the work station in front of each occupant to simulate contaminants coming from office equipment and the other is from the occupants' work activities.

2 Methods

The main objectives of the proposed LEVO air distribution system are to improve the energy saving and provide a healthy and comfortable local environment around the occupants by controlling the heat convection resulting from the room heat sources, i.e. the thermal plumes generated by the occupants and other heat sources. Fig.1. shows schematic diagrams of (a) the LEVO combined with the office workstation, (b) air flow direction around the occupants in a room using the LEVO system, (c) the details of the simulated room, and (d) the arrangement of the simulated room. A numerical investigation of the combination between the lamps and exhaust opening was performed by the current authors [21, 22]. In these publications, the impact of the combination between the room heat sources and exhaust opening on the energy saving was investigated numerically. The results showed that extra energy saving can be achieved in rooms that have combined the exhaust with lamps into one unit. While, in this study, the combination concept between the room heat sources and exhaust opening, which was proposed by the current researchers [21, 22], has been further improved to extract a large amount of the generated heat flux from the room heat sources. In addition, this concept was employed along with the local exhaust ventilation system in the current work for the investigated office room. In the LEVO system, the reading lamps and exhaust outlet are combined in one unit and located above the heat sources of the work station such as monitors, computers and occupants and at 1.6 m from the floor level (see Fig.1 a and b). In this system, the warm and contaminated air generated by the occupants and office activities are extracted locally before mixing with the rest of the air in the room. In order to improve the temperature distribution in the vertical direction and reduce the temperature differences between the foot and head levels, the extracted warm air was directed towards the foot level. A small amount of the extracted heat is transferred into the area near to the foot level (see Fig.1 b) which subsequently improves the temperature distribution in the vertical direction. This creates a healthy and comfortable work environment, especially in the area around the occupant's workstation, and causes the exhaust air temperature to increase, which leads to enhance energy saving. In this study, a detailed 3D numerical simulation was performed using the commercial software ANSYS Fluent to assess the performance of the LEVO system in providing localized thermal comfort and enhancing the air quality in the inhaled area, as well as in reducing the energy consumption of the system. For an accurate prediction of the temperature, velocity and particle concentration distribution, the numerical results were validated against the experimental results from published work [44]. In order to determine the best performance of the LEVO system in the office, three different amounts of the return air were examined using the validated numerical model. The comparison study was performed to investigate its impact on the energy saving and the indoor thermal environment with and without the LEVO system, as listed in Table 1. Since this investigation was targeted at the energy saving and the indoor thermal comfort in an office space, especially in the area around the occupants, a full scale computational domain representing a typical office with dimensions of 4 m long, 2.7 m high and 3 m wide was used in the simulation. The office heat sources include two occupants, two computer cases, two monitors, and two lamps. The office bounded walls, ceiling and floor were modelled as adiabatic. Table 2 lists the heat rate emitted from each heat source.

Two sources of contaminant were used in this study to simulate the contaminants generated by the office equipment and office work activities. The particles of 0.7 µm with density of 912 kg/m^3 were generated for each case study. This type of particle belongs to particles in the accumulation mode (0.1-2 µm) such as those found in building dust and smoke. A Displacement Ventilation (DV) system was employed in this study as the main air distribution system. With the DV system, fresh and cool air is normally supplied at or close to the floor level with low velocity. In addition, a stratification of temperatures and contaminant is formed in the room domain and the horizontal temperature profile is uniform except for the region near the DV supply diffuser and room heat sources, which may help to improve the indoor thermal environment [23]. A supply DV diffuser (1.0 m ×0.6 m) was located at the floor of the side wall and the return opening (0.8 m × 1.0 m) was located at the upper boundary of the occupied area, 1.3 m from the floor level (see Fig.1 d), as recommended by Cheng et al. [24]. The set room temperature in the occupied zone was 24°C for all case studies. The total supply air velocity was 0.14 m/s, and its temperature was 19 °C.

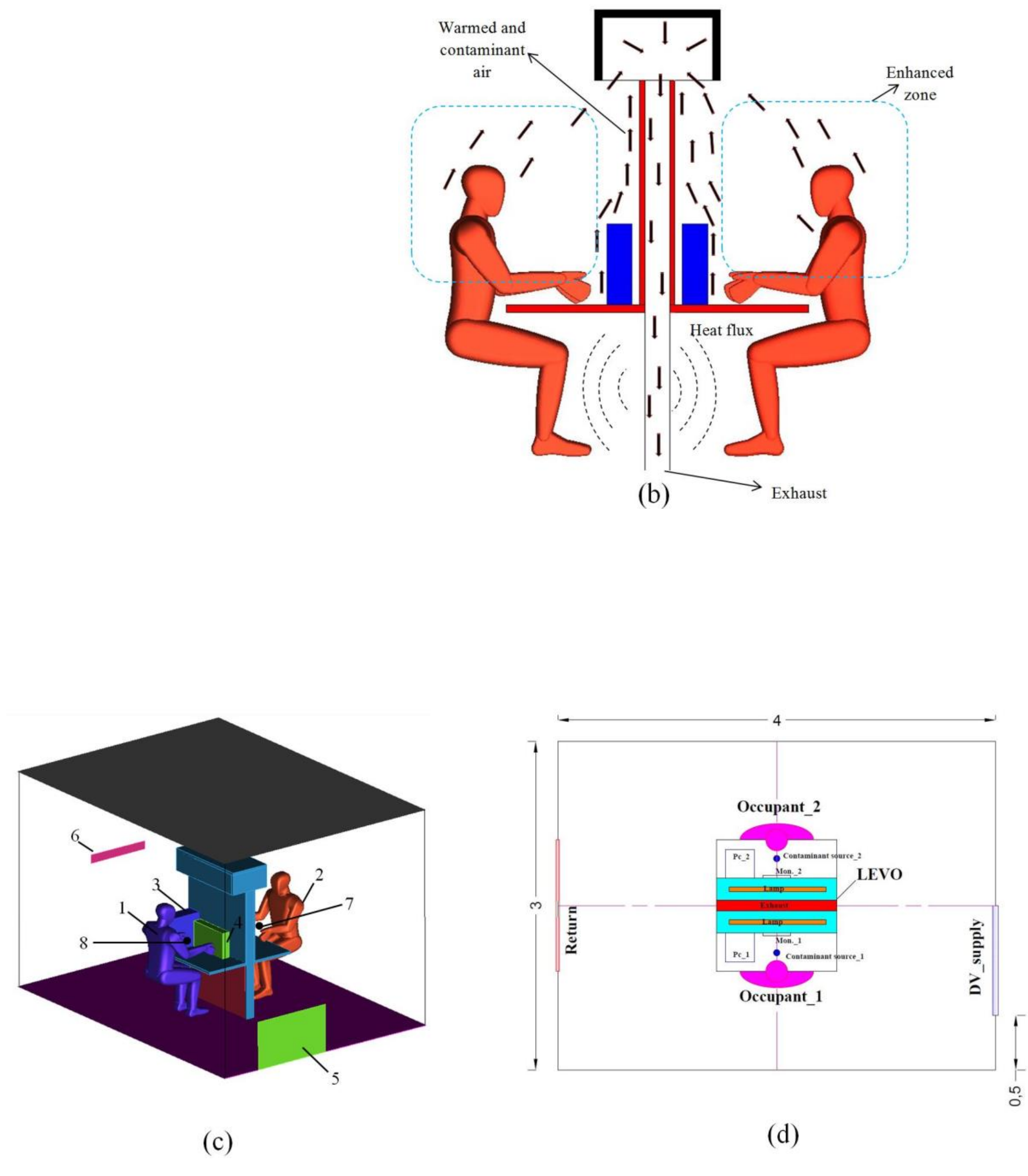

Fig. 1. (a) LEVO system parts: 1- lamps, 2 - air suction part, 3 - exhaust inlet and 4 - table; (b) LEVO system combined with the office heat sources and air flow direction; (c) Configuration of the simulated room: 1 - occupant 1, 2 - occupant 2, 3 - PC case, 4 - PC monitor, 5 - DV inlet, 6 - return inlet, 7 - contaminant source 1 and 8 - contaminant source 2; (d) The equipment arrangement of the simulated office.

Table 1

Case studies.

Case study	Return air percentage
Case 1	35% (return velocity = 0.35 m/s).
Case 2	50% (return velocity = 0.50 m/s).
Case 3	65% (return velocity = 0.68 m/s).

Table 2

Cooling load for the simulated office room.

Internal heat sources.	Cooling load
Occupants	60×2 (W)
PC case	60×2 (W)
PC monitor	70×2 (W)
Lamps	24×2 (W)
Total	428 (W)
Heat flux density based on the floor surface area	35.67 W/m^2

2.1 Grid independence test

As a result of the human body and the room equipment complexity, a tetrahedral unstructured mesh with inflation boundary layers around the occupants was generated using ANSYS ICEM CFD software. The meshes around the occupants and others heat sources were fine enough to capture the heat convection behaviour and to satisfy the y^+ values requirement. The mesh was clustered in regions that have high temperature and velocity gradients such as walls, equipment and table. To resolve the boundary layer around the occupants, an inflation boundary layer of 5 layers was generated with a growth rate of 1.2 and the first layer thickness was 1.5 mm. The y^+ values of $0.7 \leq y^+ \leq 4.5$ was achieved (see Fig. 2). The grid independence test plays an important role in a CFD simulation regarding results accuracy and prediction cost. In the current study, the proper grid size was selected by comparing the simulation results from three different sizes of mesh as listed in Table 3. By increasing the grid cells from mesh_2 to mesh_3, there is no significant change in the predicted temperature and velocity distributions. Therefore, mesh_2 was selected to be the adequate mesh size for the rest of the simulations.

Table 3

Mesh independence test.

Mesh types.	Cells number
mesh_1	1,518,077
mesh_2	2,753,932
mesh_3	3,493,875

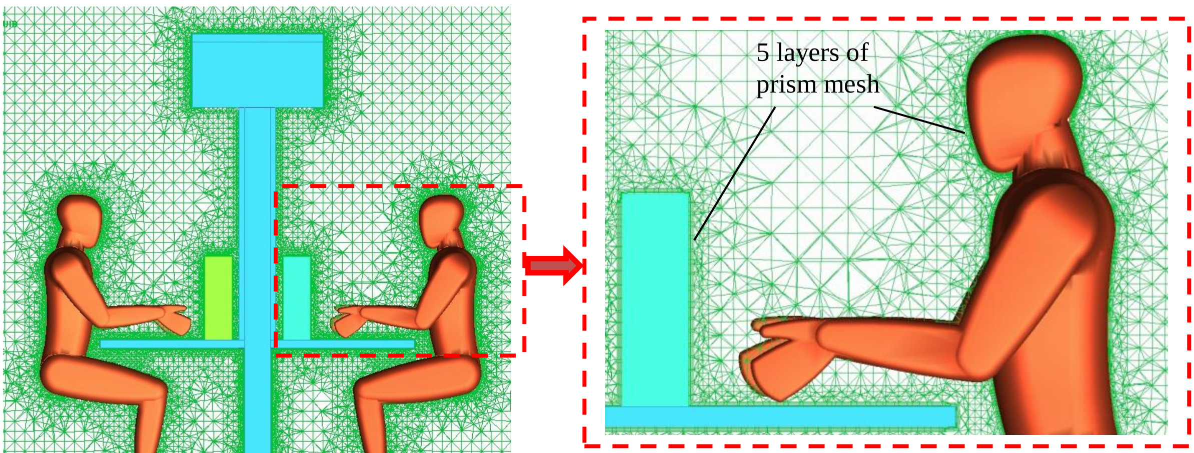

Fig. 2. Inflation boundary layer around the human body.

2.2 Air flow modelling

For an accurate prediction of indoor air distribution and contaminant dispersion, a suitable turbulence model needs to be used. The two–equation renormalized group (RNG) $k-\varepsilon$ turbulence model was selected to predict the flow and thermal fields characteristic in the office room. This model produces an accurate prediction of the indoor thermal environment and contaminant distribution [25-28]. All the detailed equations can be found in the references [29, 30].

The CFD ANSYS©FLUENT R 15.0 software was employed to solve the Reynolds averaged Navier-Stokes equations and calculate the Lagrangian trajectories in the 3D computational model of the office room. The enhanced wall treatment with reasonable y^+ value was applied to the regions near the solid surfaces. The Boussinesq assumption was used to calculate the change in air density due to the temperature variations. The semi-implicit method for pressure-linked equations (SIMPLE) algorithm was selected for pressure and velocity coupling, and the upwind second order discretization scheme was used for all the terms in the equations except for the pressure, which was solved by using a staggered scheme named pressure staggering option (PRESTO!). In the present work, the discrete ordinates (DO) model [31] was employed to simulate the radiation heat emitted from internal heat objects which included two occupants, two monitors, two computers and two reading lamps. Table 4 summarized the details of the numerical methods and boundary conditions for this study.

Table 4

Details of numerical methods and boundary conditions.

Turbulence model	Renormalized group RNG $k-\varepsilon$ turbulence model.
Radiation model	Discrete ordinates (DO) radiation model.
Numerical schemes	For pressure, staggered third order scheme PRESTO!; for other terms, upwind second order; SIMPLE algorithm.
Ceiling, floor, tables and bounded walls	Adiabatic wall
Supply air	Velocity inlet (0.14 m/s, 19 °C)
Exhaust	Pressure –outlet
Occupants	Uniform heat flux 60 W × 2
Pc case	Uniform heat flux 60 W × 2
Pc monitor	Uniform heat flux 70 W × 2
Lamps	Uniform heat flux 24 W × 2

2.3 Discrete Phase Modelling (DPM)

Generally speaking, particle distribution can be predicted using either the Eulerian-Eulerian or the Eulerian-Lagrangian approach for the steady state particle distribution indoor [32]. In current study, an Eulerian-Lagrangian approach, named as discrete phase model (DPM), was employed to track the particles trajectory through the fluid phase. The Eulerian approach was employed to simulate the continuous phase (fluid phase), while the Lagrangian approach was employed to simulate the discrete phase (airborne particles). The fluid phase was treated as a continuum and solved using the Reynolds averaged Navier-Stokes equations, while the discrete phase was solved by tracking individual particles trajectory through the air flow field. Due to the particle volume fraction was sufficiently small, the interaction between the fluid phase and discrete phase was assumed to be by one way coupling; i.e. the particles were affected by the drag and turbulence of the airflow but there was no effect of the particles on the fluid phase [30]. There are three modes of particle size: ultrafine (< 0.1μm); accumulation (0.1-2 μm) and coarse (> 2 μm) [33]. In order to simulate the contaminant distribution generated by office equipment and office work activities, this study employed accumulation mode to predict the contaminant concentration distribution in the breathing zone and the quality of the inhaled air.

2.3.1 Particles tracking equations

The Lagrangian approach was employed to calculate the individual trajectories of each particle by solving the momentum equation. By equating the particle inertia force to the external forces, the momentum equation can be written as:

$$\frac{d\vec{u}_p}{dt} = F_D\left(\vec{u} - \vec{u}_p\right) + \frac{\vec{g}(\rho_p - \rho)}{\rho_p} + \vec{F}_a \tag{1}$$

where the inertial force per unit mass $(m\, s^{-2})$ term is expressed on the left-hand side of Eq. (1). The drag forces per unit mass are represented by the first term of the right hand side. The gravitational and buoyancy forces are expressed by the second term; $\vec{F}_a$ is employed to add the additional forces (per unit mass) which may have an influence on particle motion. In the present study, the drag force is the important force acting on the particles motion and follows the Stokes drag law:

$$\vec{F}_{drag} = F_D\left(\vec{u} - \vec{u}_p\right) = \frac{18\mu}{\rho_p d_p^2\, C_c}\left(\vec{u} - \vec{u}_p\right) \tag{2}$$

where C_c is the Cunningham correction factor which is calculated from the following equation:

$$C_c = 1 + \frac{2\lambda}{d_p}\left(1.257 + 0.4e^{-(1.1d_p/2\lambda)}\right) \tag{3}$$

In the current study, the Basset history, the pressure gradient and virtual mass were negligible or had no significant impact compared to the drag force. In ventilated rooms, the Brownian motion, thermophoretic and Saffman's lift are two orders of magnitude smaller than the Stokes drag force and occasionally these forces become compatible with Stokesian drag force when a very small size particles are used in flow field [34]. The Brownian motion and Saffman lift forces may become considerable and affect the particle motion [30, 35, 36], especially in the turbulent boundary layer near to the wall regions [35]. In addition, these forces play an important role in the deposition process [37-39]. Therefore, they were taken into consideration in the current work. The final form of trajectory equation becomes:

$$\frac{d\vec{u}_p}{dt} = F_D\left(\vec{u} - \vec{u}_p\right) + \frac{\vec{g}(\rho_p - \rho)}{\rho_p} + \vec{F}_b + \vec{F}_{thermal} + \vec{F}_s \tag{4}$$

In a turbulent flow, the particle path is significantly influenced by local turbulence intensities. In order to simulate the stochastic velocity fluctuations in airflow, the discrete random walk (DRW) approach was employed in this work [40]. The instantaneous velocity is expressed by the time-averaged flow field velocity $\bar{u}_i$ and fluctuating velocity $u_i^{'}$. The final form of the fluctuating velocity components can be expressed as:

$$u_i' = \xi_i \sqrt{\bar{u}_i'^2} = \xi_i \sqrt{2k/3} \tag{5}$$

Due to the assumption of one way coupling between the two phases, the air flow field is solved first, and then the particles are injected [41]. As mentioned previously, the air flow equations and Lagrangian trajectories of the particles were solved using ANSYS Fluent software. However, the Lagrangian approach does not calculate the concentration of the particles in the fluid domain directly. Therefore, a user-defined function (UDF) was used to calculate the concentration distribution of the particles from the trajectories. In order to calculate the particle concentration in the fluid flow phase, it is necessary to correlate the concentration with the trajectories for each computational cell in the domain. This can be achieved using particle source in-cell (PSI-C) method based on the equation (6):

$$C = \frac{\dot{m} \sum_{i=1}^{n} dt(i,j)}{V_j} \tag{6}$$

The accuracy and the stability of the Lagrangian model was studied by Zhang and Chen [32]. In this study, a sufficient number of trajectories are required to get a statically stable calculation of the particle concentration in the room domain [42].Therefore, for the stable calculations of the particle concentration, an adequate numbers of particle trajectory have been tracked in the room domain.

2.3.2 Boundary conditions

Particles may escape and their trajectories terminate when they reach the inlets and exhaust opening in the room domain. When particles reach rigid objects, they may attach to or rebound from the outer surface of these rigid objects. For ventilated room, particles are most likely to attach to the solid objects surface indoor because they do not have sufficient energy to rebound to overcome adhesion [43]. When the grid at the walls region is not fine enough, the computed results will over predict. The viscous sub-layer kinetic energy and the fluctuating velocity will increase in these areas near the walls, which will increase the collision of particles with the walls. In this study, an inflation boundary layer was employed in the regions near the walls to provide the required near-wall mesh refinement. Therefore, the particle collisions in these regions were calculated accurately.

3 Model validation

3.1 Air velocity and temperature validation

In order to evaluate the CFD model validity of the current study, the simulation results for velocity and temperature distribution were compared with the published experimental data from Xu et al. [44]. In their study, an experimental study on air velocity distribution and temperature distribution in a room environment was performed. The study was performed in a small office room with dimensions of 6.0 m long, 3.9 m wide, and 2.35 m high and two heat sources included one occupant (76 W) sat in front of the table and one computer (40 W) located on the centre of the table. Figs. 3 (a) and (b) show schematic diagrams of the experimental chamber and the arrangement of the measured location respectively. Three poles, pole 2, 4 and 5, were used in this validation to predict the velocity and temperature distribution (see Fig. 3 b). The dimensions of the supply and exhaust diffuser were 0.4 m × 0.15 m and 0.34 m × 0.14 m respectively. The supply air flow rate was 43 m^3/h. The supply air temperature was 19 °C. Different temperature values were used for the bounded walls, ceiling and floor. Figs. 4 and 5 show comparisons between the experimental and simulated results for air velocity and temperature distribution respectively at three different pole positions. A good agreement between the experimental and simulated results can be seen from these figures. All other details on the room geometry and flow boundary condition can be found in Xu et al. [44].

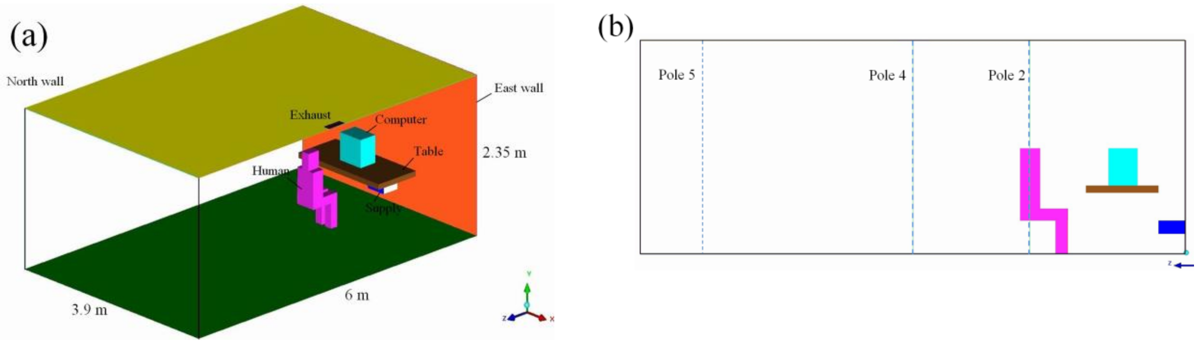

Fig. 3. (a) Schematic diagram of the experimental chamber for validation [44]; (b) The arrangement of the measured locations.

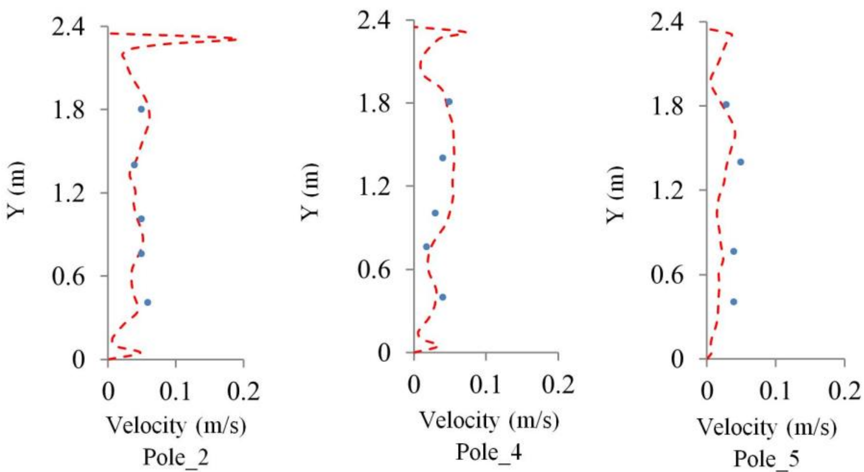

Fig. 4. Comparison of measured and simulated velocity profiles (circular symbols: experimental velocity [44]; dashed line: simulated velocity).

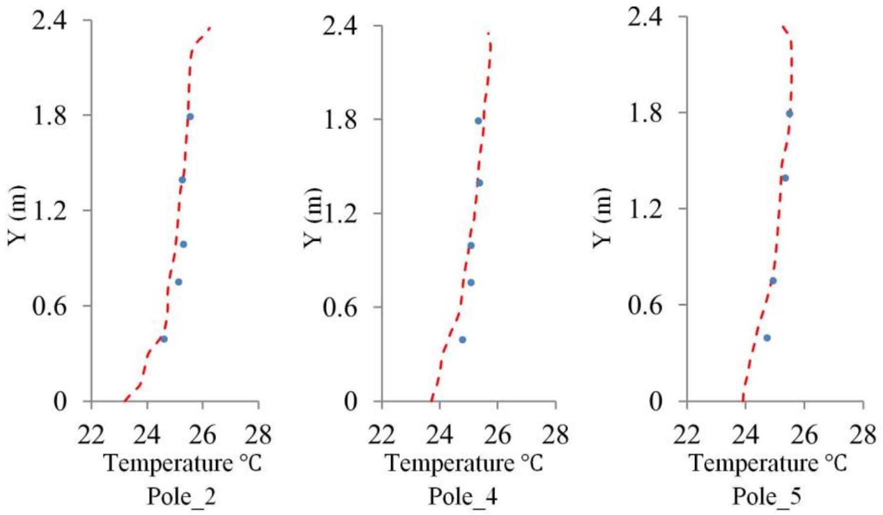

Fig. 5. Comparison of measured and simulated temperature profiles (triangle symbols: experimental temperature [44]; dashed line: simulated temperature).

3.2 Particle concentration validation

In order to validate the Lagrangian particle-tracking model, the published experimental data of Chen et al. [45] are used to test the accuracy and the efficiency of this model. Fig. 6 shows the schematic diagram of the experimental chamber with dimensions of 0.8 m × 0.4 m × 0.4 m. The inlet and the outlet diffusers had the same dimensions (0.04 m × 0.04 m) and were centred about the mid-space plane of the test room (see Fig. 6). The supply air velocity was 0.225 m/sec and the particle diameter and density were 10 μm and 1400 $\mathrm{kg/m^3}$ respectively. The concentration of particle was normalised by the concentration at the inlet.

Fig. 7 shows the comparison between the normalised particles concentration and the experimental data at three different locations. A reasonable agreement between the predicted results and experimental data can be seen from these figures.

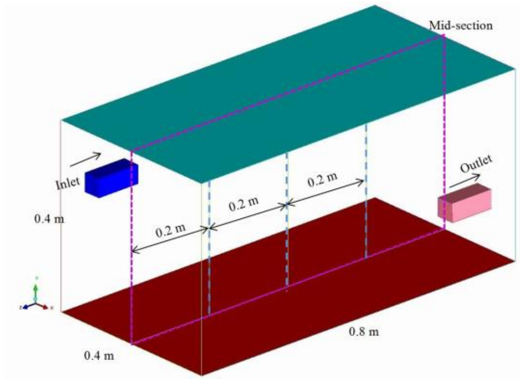

Fig. 6. Schematic diagram of ventilated chamber for the validation of Lagrangian particle-tracking [45].

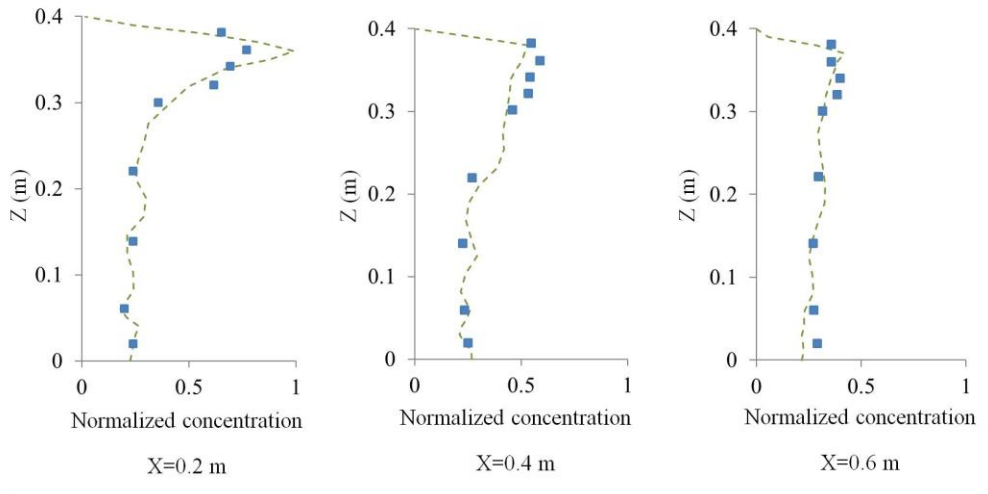

Fig. 7. Comparison between the normalized particle concentration and experimental results [45] at three different locations x = 0.2, 0.4 and 0.6 (square symbols: experimental data [45]; dashed line: predicted normalized particle concentration).

4 Results and discussion

4.1 Indoor thermal comfort

The indoor human thermal comfort indices are evaluated using Fanger's comfort equations [46]. In this model, the thermal balance for the whole human body is expressed by two indices, the predicted mean vote (PMV) and the predicted percentage of dissatisfied (PPD). The PMV parameter refers to the mean value of the votes of people in the same thermal environment on a seven-point thermal sensation scale as shown in Table 5. In this index, the four physical variables (air temperature, mean radiant temperature, air velocity and relative humidity) and two personal variables (clothing and people activity) are used to predict the human thermal comfort conditions in the occupied zone. The PPD is an index which refers to the percentage of people in a large group who are prone to be thermally dissatisfied under specific thermal conditions, and is calculated from the PMV parameter. For the indoor human thermal comfort requirement, suitable PMV and PPD values are in the range of $-0.5 < PMV < 0.5$ and PPD < 15% respectively. For good indoor human thermal comfort, small PPD and PMV values are highly recommended. The detailed PMV and PPD equations can be found in the reference [46]:

Table 5
The relation between PMV and thermal sensation

PMV	Thermal sensation
+3	Hot
+2	Warm
+1	Slightly warm
0	Neutral
-1	Slightly cool
-2	Cool
-3	Cold

The PMV and PPD indices were used to assess the human thermal comfort in each case study. The comparison between the PMV and PPD results for both occupants in the investigated room with and without the LEVO system are listed in Table 6. In this step, three different amounts of recirculated air were examined (see Table 1). In cases 1, 2 and 3, the PMV and PPD indices for the room with and without the LEVO system (reference case) were approximately the same with only a slight difference between them; this was due to the fact that the air temperature and velocity in the area near foot level, shown in Fig. 8, was slightly increased compared with the room without the LEVO system (see Fig. 8), which subsequently affected the thermal environment in these regions. Similar findings were reported by Horikiri et al. [47]. For all cases, the thermal comfort indices for occupant 1 were slightly better than for occupant 2. This was because the position of occupant 1 was slightly further away from the inlet supply diffuser, temperature and air velocity. It can be conclude that, the above results show that there is no significant improvement of the indoor thermal environment regarding to PPD and PVM. However, the other results show that with LEVO, a significant improvement with an acceptable thermal comfort was achieved regarding to the other evaluation parameters such as vertical temperature distribution, air quality in the occupied zone as well as energy saving.

Table 6
PMV-PDD indices for each case study and for both occupants

Case study	Occupant_1				Occupant_2			
	Ref.		LEVO		REF		LEVO	
	PMV	PDD	PMV	PDD	PMV	PDD	PMV	PDD
Case_1	-0.34	7.50	-0.33	7.50	-0.33	7.0	-0.33	7.5
Case_2	-0.33	7.25	-0.3	7.25	-0.31	7.0	-0.28	6.5
Case_3	-0.33	7.25	-0.31	7.25	-0.28	6.5	-0.27	6.5

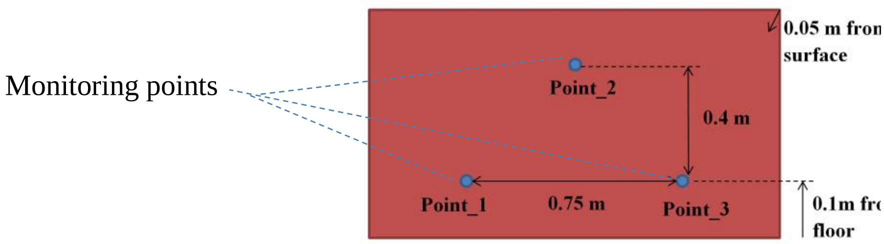

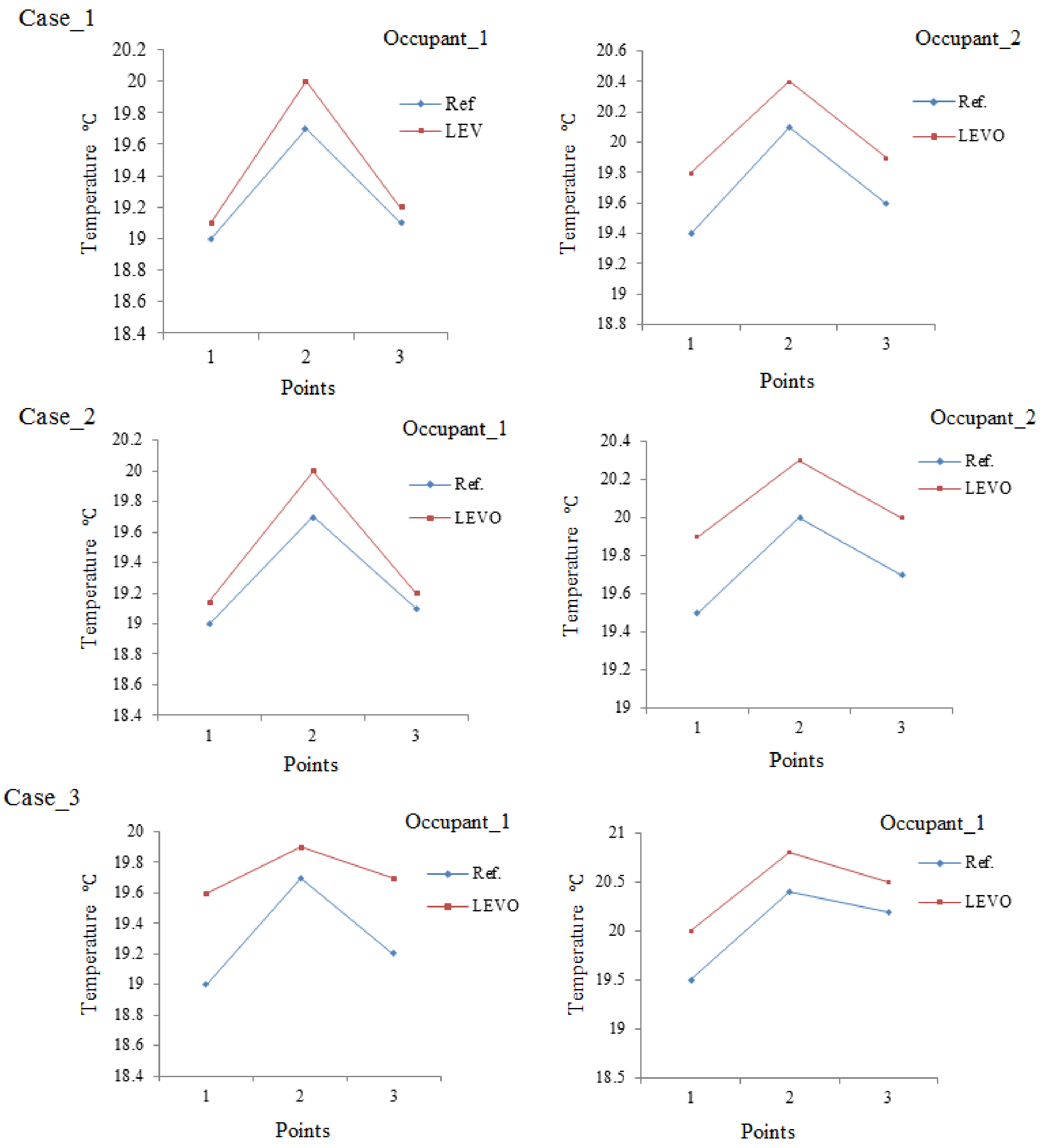

Fig. 8. Temperature distribution (°C) of the near foot zone at three monitoring points, point 1, 2 and 3, for each case study and for both occupants.

It is thus concluded that the impact of the heated area near the foot level on thermal comfort around the seated occupants is not very significant, other than a slight enhancement of PVM and PPD indices (see Table 6). In addition, for all data the PMV index was between -0.3

and -0.36, while the value of PPD index was between 6.5 and 7.5. These indicate that the room was observed to be between neutral and slightly cool (see Table 5) and still within the thermal comfort range.

4.2 Temperature distribution in the vertical direction

The temperature gradient in a vertical direction is one of the major factors in evaluating indoor thermal comfort in a stratified air distribution (STARD) system. As recommended by the ASHRE standard [48], the temperature difference between the head level, 1.1 m high from the floor level, and the foot level, 0.1 m high from the floor level, should not exceed 3℃. In the current study, the local thermal discomfort index ($\Delta T_{head-foot}$) was evaluated in the region around the occupants. As shown in Fig. 9 (a), four positions (points 1, 2, 3 and 4), two points at each occupant, were used in the current study to assess the thermal discomfort in each case. In cases 1, 2 and 3, it is clear to see that using the LEVO system improved the temperature distribution in the vertical direction in all locations compared with the room in which the system was not used (see Fig. 9 b, c and d). This is because the LEVO system works to extract the warm air in the vicinity of the occupant and directs it towards the foot level. This process leads to a reduction in the air temperature at the head zone and slightly increased air temperature at the foot level which subsequently reduced the temperature differences, ($\Delta T_{head-foot}$), and improved human thermal comfort. In addition, the local extraction of the heat generated by the room heat sources using the LEVO system improved the temperature differences between the upper and lower parts of the room. Fig.10 shows the temperature and velocity distribution for (a) using the LEVO system and (b) for the reference case (without using the LEVO system). The temperature differences, ($\Delta T_{head-foot}$), at points 1 and 2 were slightly higher than the others; the reason for this is that the positions of these points were close to the supply inlet diffuser. Similar findings were revealed by Lian and Wang [49]. It can be concluded that a good enhancement of human thermal comfort was achieved by locally extracting the warm air generated by the room heat sources using the new LEVO system.

A clearer representation of temperature distribution in the vertical direction, as given in Fig. 11, along four vertical poles passing through the monitoring points, 1, 2, 3 and 4 (see Fig. 9 a). From this figure, it is possible to note that the temperature difference between the upper and lower parts of the room was reduced by using the LEVO system. This was due to the fact that the LEVO system extracted the warm air generated by the room heat sources locally at the work station before mixing with the rest of the room air. Similar findings were reported by the current authors [21, 22]. This process contributed to reducing the temperature differences between the upper and the lower parts of the room, which subsequently created a more homogenous distribution of the temperature in the room (see Fig. 10).

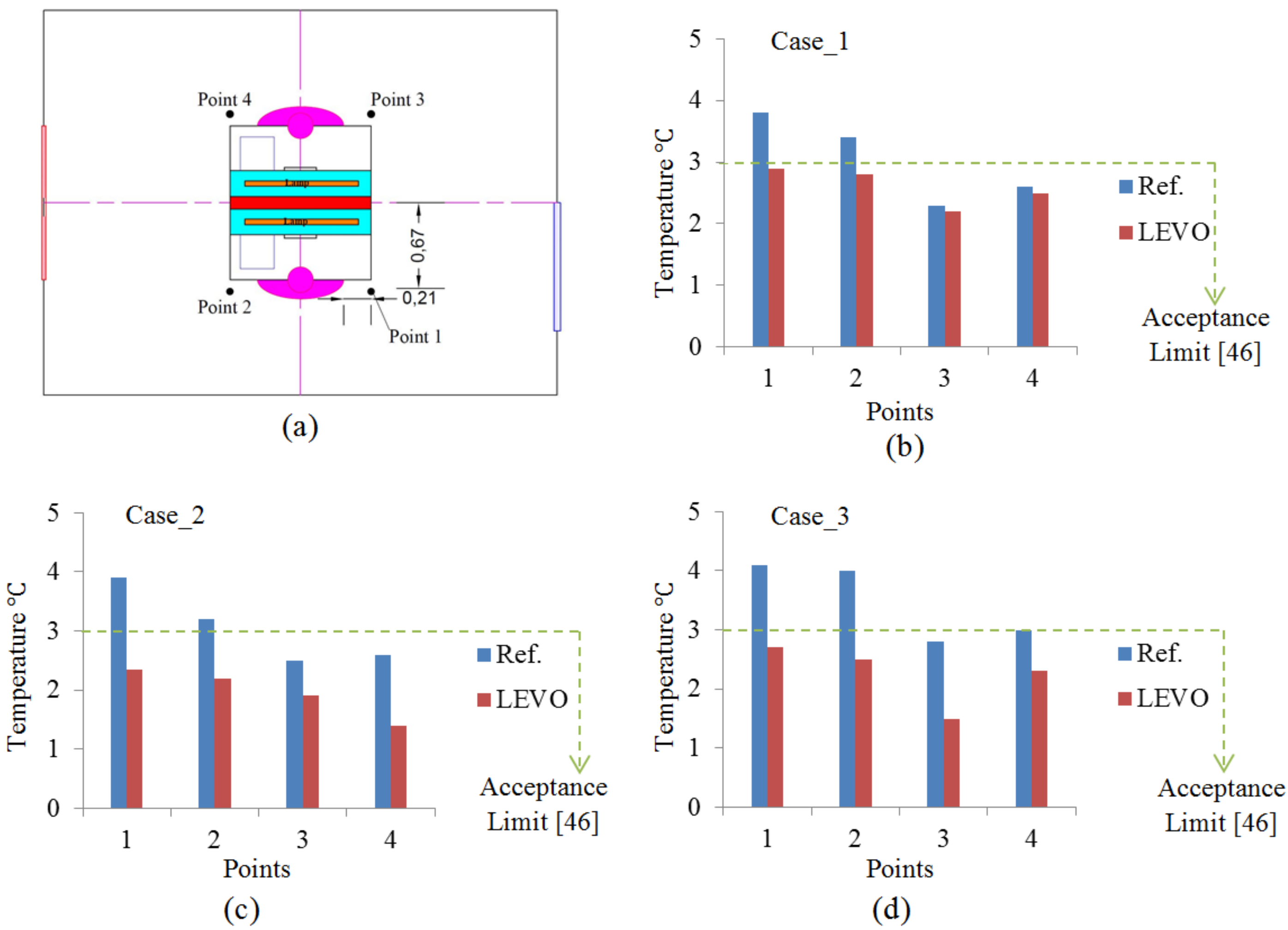

Fig. 9. (a) Monitoring points; (b), (c) and (d) Temperature gradient (℃) in vertical direction for each case study.

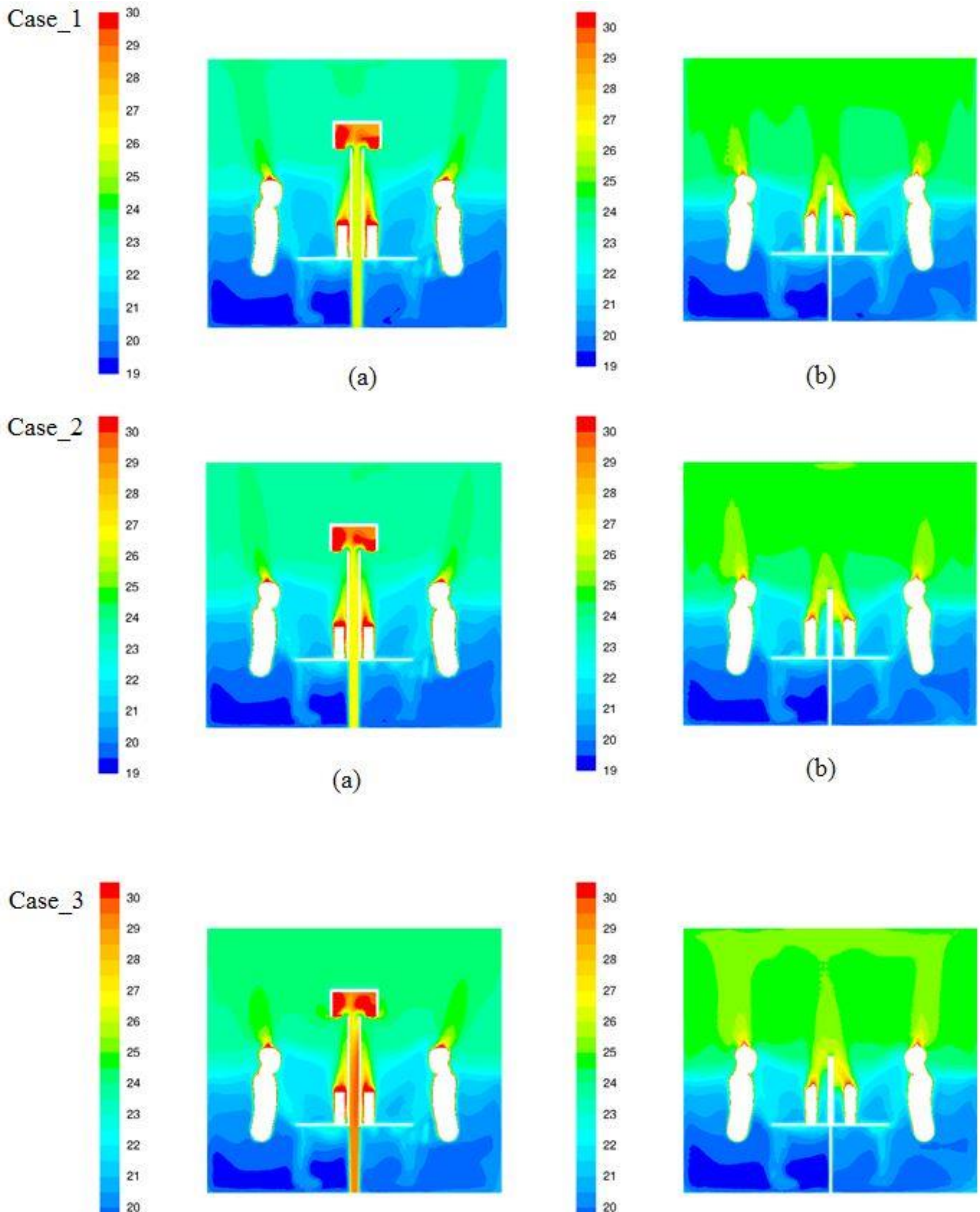

Fig. 10. Temperature (°C) at the mid plane (x=2m) for each case study (a) with LEVO and (b) without LEVO as the reference.

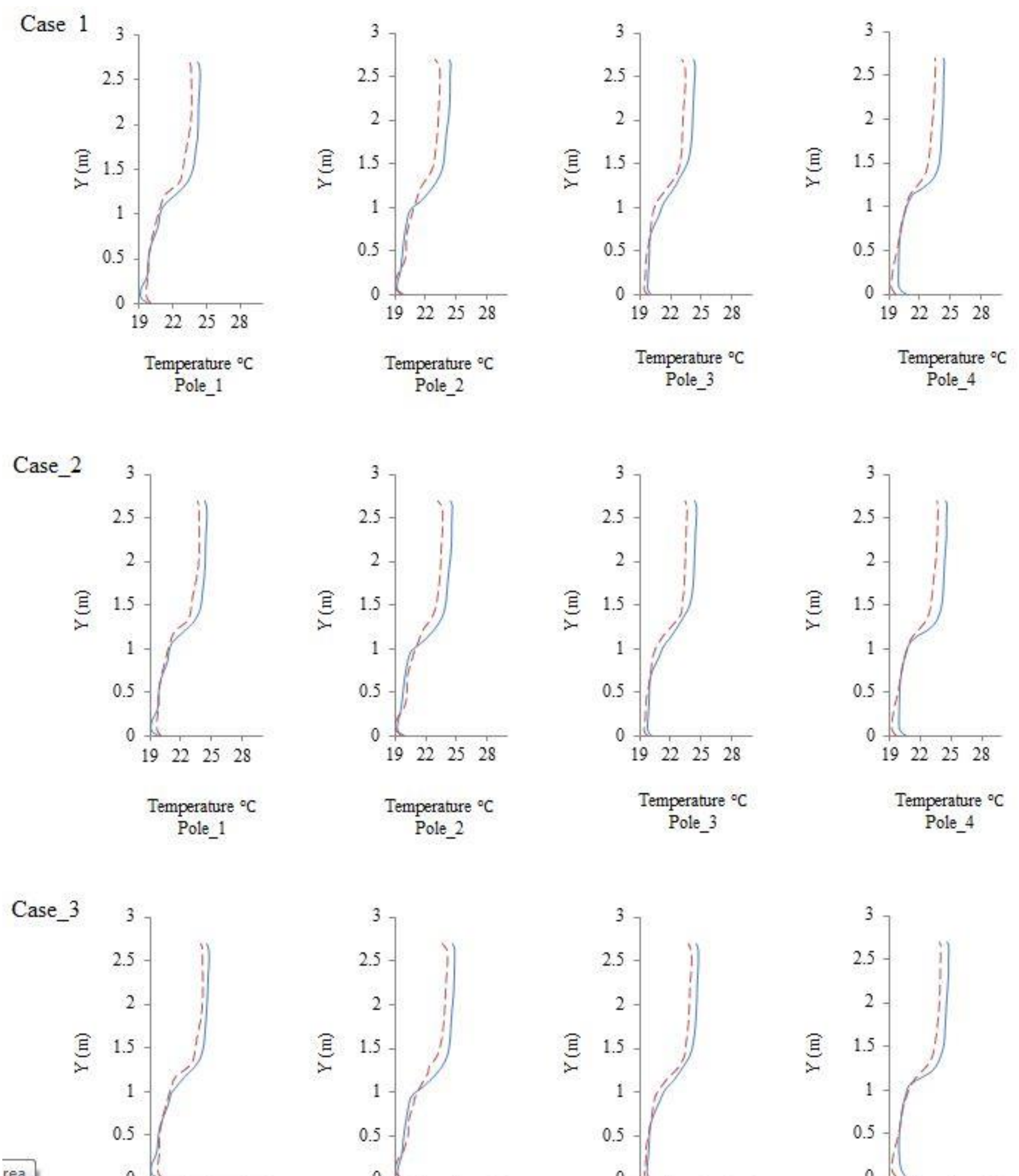

Fig.11. Temperature gradient in vertical direction for each case study.

4.3 Energy saving evaluation

For the Stratified Air Distribution (STRAD) system, only the occupied zone is required to be thermally comfortable, which enhances the potential to increase energy saving. The energy savings were evaluated in this study to show the impact of using the LEVO system on energy consumption. Cheng et al. [24] developed a method to evaluate the energy saving in a room using a STRAD system by calculating the reduction in cooling coil load that is based on the CFD simulation results. For the same room set temperature (T_{set}), the calculation of cooling coil load in a room using the STRAD system is different from that in the mixing ventilation (MV) system:

$$Q_{coil-STRAD} = Q_{coil-MV} - c_p \times \dot{m}_e \times (T_e - T_{set}) \tag{7}$$

$$Q_{coil-MV} = Q_{space} + Q_{vent} \tag{8}$$

where $\dot{m}_e$ and T_e refer to the exhaust air mass flow rate and exhaust temperature respectively and T_{set} represents the room set temperature which was 24°C for all the case studies. The amount of cooling coil load reduction in the STRAD system is presented in term of $c_p \times \dot{m}_e \times (T_e - T_{set})$. This term was used in the present work to evaluate the efficiency of the LEVO system regarding to the energy saving for each case.

Table 8 illustrates that the reduction in the cooling coil load and the amount of energy saving are proportional to the exhaust temperature (T_e) and the exhaust mass flow rate ($\dot{m}_e$).

In cases 1, 2 and 3, a significant improvement in energy saving was obtained in the office room using the LEVO system compared with the reference case for each case study. The enhancement of energy saving in cases 1, 2 and 3 was calculated by comparing to the reference case (see Table 8). This is because the local extraction of the heat generated from the heat sources contributed to an increase in the exhaust air temperature, consequently enhancing the potential of energy saving. As mentioned previously, the energy savings are directly related to the exhaust mass flow rate ($\dot{m}_e$). As illustrated in Table 8, the energy saving enhancement was improved by decreasing the exhaust mass flow rate ($\dot{m}_e$) for cases 1, 2 and 3. Correspondingly, the energy saving improvement increased by reducing the exhaust mass flow rate in the room with the LEVO system from 22.56 % in case 1 to 26.6% in case 2 and to 30.4 % in case 3. This is due to the fact that by increasing the exhaust mass flow-rate a small amount of fresh air may be extracted directly by the LEVO system which reduces the exhaust air temperature and subsequently reduces the energy saving. From these results, it can be conclude that energy saving depends on the exhaust temperature and exhaust mass flow-rate; i.e. extra energy saving can be achieved by increasing the exhaust air temperature and decreasing the amount of the exhaust mass flow rate. In energy saving evaluation, other factors such as thermal comfort indices, temperature gradient in the vertical direction and contaminant concentration distribution should also be considered carefully.

Table 8
Energy saving for cooling coil for each case study.

	Case_1		Case_2		Case_3	
	Ref.	LEVO	Ref.	LEVO	Ref.	LEVO
Exhaust air temperature $T_{exhaust}$ (°C)	24.3	25.4	24.4	26.2	24.6	27.6
Return air temperature T_{return} (°C)	23.1	22.3	23.3	22.6	23.4	22.8
ΔQ_{coil} (W)	21.7	96.5	20.6	113.7	21.7	130.2

$\Delta Q_{coil}/Q_{space}$ (%)	5.07	22.56	4.8	26.6	5.0	30.4

4.4 The quality of the indoor air in breathing and inhaled zones

The IAQ plays an important role in the assessment of indoor air distribution system performance, especially in terms of distribution and contaminants concentration. One of the most important factors affecting indoor particle concentration distribution is the position of exhaust diffusers and contaminant sources. In the current study, the contaminant sources were located at the work station (see Fig. 1) to simulate the contaminants generated by the office equipment and office work activities. The quality of the occupants' inhaled air was evaluated in the inhaled area around the occupants' heads (see Fig. 13 a). In addition, the air quality in the breathing zone was evaluated at 1.3 m above the floor. For this study, the contaminant concentration normalisation is defined as:

$$C_n = \frac{C_p}{C_e} \quad (9)$$

where C_n is the normalised concentration, and C_p and C_e are the contaminant concentration in a specific region and the concentration at the exhaust respectively.

Figs. 13 b, c and d compare the normalised particle concentration for each case in the breathing level and inhaled zone respectively. From these figures it can be noted that the quality of the indoor air was improved significantly in the room using the LEVO system in both the breathing and the inhaled zones. Fig. 13 b shows the quality of the indoor air at the breathing level for the room with and without the LEVO system for each case study. Cases 1, 2 and 3 show that no noticeable change in the contaminant concentration with changing the return air velocity without LEVO. However, using the LEVO system enhanced the quality of the indoor air significantly (see Fig. 13 b). This was because a large amount of the generated contaminants was extracted directly from the LEVO system before it could disperse into the breathing or the inhaled zones. In addition, the thermal plumes generated by the heat sources which are located near the LEVO system bring an additional amount of contaminant to be extracted from the system [50]. This improved the quality of the indoor air in both the breathing and the inhalation zones (see Figs. 13 b, c and d). In case 1, the concentration of the contaminant in the breathing level was larger than those in cases 2 and 3 by 13%. The reason for this was that the mass flow rate of the exhaust in case 1 was low and this led to a reduction in the amount of extracted contamination at the breathing level and consequently increased the contaminant concentration compared to cases 2 and 3. For the inhaled zone, it is clear that the inhaled air quality for occupant 1 was better than that for occupant 2 in all cases. The reason for this is that the position of occupant 1 was located close to the DV supply. This caused the velocity of the supply air to be able to drive the contaminant away from the inhaled zone of occupant 1, which helped to improve the air quality in this zone compared to occupant 2. This is consistent with findings reported by Sadrizadeh and Holmberg [51]. From these results it can be concluded that by using the LEVO system the quality of the indoor air in the breathing zone was improved significantly compared to the reference case by 45 %, 59.6 % and 61.4 % for cases 1, 2 and 3 respectively (see Fig. 13 b). Furthermore, compared with the reference case, the use of the LEVO system contributes to reducing the contaminant concentration in the inhaled zone significantly for both occupants (see Figs. 13 c and d).

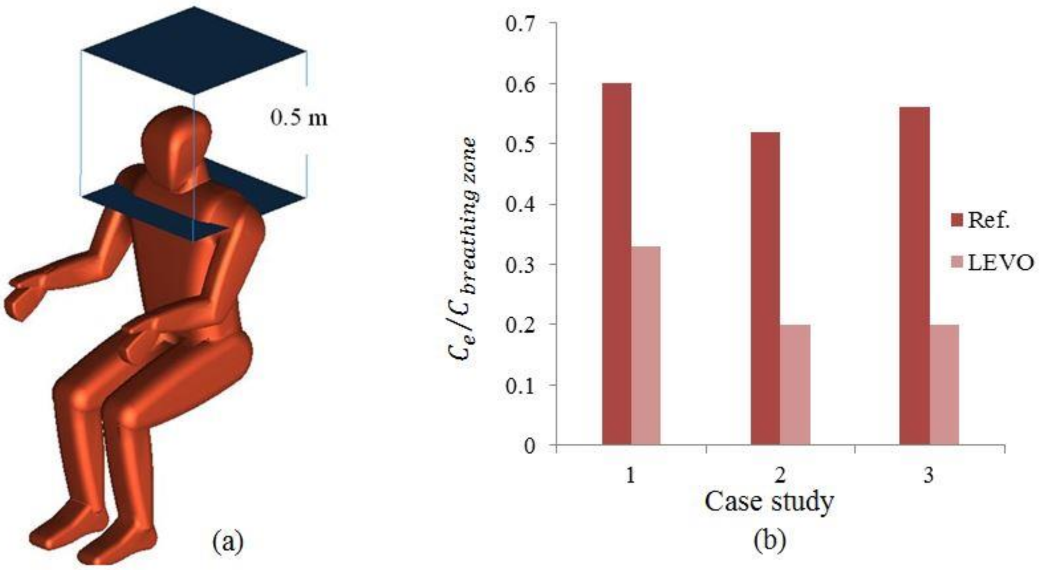

Fig. 13. Comparison of the quality of indoor air for each case study; (a) inhaled zone; (b) contaminant concentration at breathing level; (c) and (d) the inhaled air quality for occupant_1 and occupant_2 respectively.

5 Conclusion

In this study, the influences of using a novel LEVO system on the thermal comfort, the quality of the room air in the inhaled zone and the breathing zone and on the energy saving were numerically investigated in a typical office room served by a DV system. The performance of the LEVO system was evaluated for different amounts of return air. Contaminants generated by office work station equipment and occupant activity were simulated. The results from this study concluded that

- Using the new LEVO system can provide a healthy and comfortable environment for the occupants compared with a room which does not use this system. The air quality in the breathing zone was significantly improved by 45%, 59.6% and 61.4% for cases

1, 2 and 3 respectively by using the LEVO system. Furthermore, this system contributed to reducing the contaminant concentration in the inhaled zone for both occupants. This was due to the fact that most of the generated contaminant at the office workstation was extracted locally via the LEVO system before reaching and mixing with the air in the occupied zone.

- Directing the extracted warm air towards the foot level had a slight impact on improving the temperature distribution in the vertical direction and subsequently contributed to improving the human thermal comfort in terms of the temperature differences between the head and foot levels.
- Using the LEVO system contributed to reducing the amount of energy consumption of the cooling coil by up to 30% compared with the reference case. This was due to the fact that most of the room heat flux generated by office work station equipment and occupant were extracted directly before it could mix with the rest of the room air, which subsequently increased the exhaust air temperature and significantly reduced the energy consumption by cooling coil. In this system, the energy saving efficiency was increased by reducing the exhaust mass flow rate. In case 3, up to 30% of energy saving was achieved compared to 22.5% and 26.6% for cases 1 and 2 respectively.
- The evaluation of energy saving alone was not meaningful, therefore other factors should be considered in the same time. Thus, the thermal comfort indices PMV-PPD, temperature distribution in the vertical direction, and the room air quality were investigated along with energy saving in this study.
- Using the concept of the LEV in an office application provided a better indoor thermal environment in terms of thermal comfort, temperature distribution, quality of indoor air, inhaled air and energy saving.

6 Acknowledgements

The authors would like to thank the Ministry of Higher Education and Scientific Research of Iraq for the financial support of the project.

References

[1] Guo H, Lee S, Chan L, Li W. Risk assessment of exposure to volatile organic compounds in different indoor environments. Environmental Research. 2004;94:57-66.

[2] Klepeis NE, Nelson WC, Ott WR, Robinson JP, Tsang AM, Switzer P et al. The National Human Activity Pattern Survey (NHAPS): a resource for assessing exposure to environmental pollutants. Journal of exposure analysis and environmental epidemiology. 2001;11:231-52.

[3] Maio S, Simoni M, Baldacci S, Sherrill D, Viegi G. Indoor air pollution and airway disease. Allergy Frontiers: Epigenetics, Allergens and Risk Factors: Springer; 2009. p. 387-401.

[4] Calay RK, Wang WC. A hybrid energy efficient building ventilation system. Applied Thermal Engineering. 2013;57:7-13.

[5] Chemisana D, López-Villada J, Coronas A, Rosell JI, Lodi C. Building integration of concentrating systems for solar cooling applications. Applied Thermal Engineering. 2013;50:1472-9.

[6] Fong K, Chow TT, Li C, Lin Z, Chan L. Effect of neutral temperature on energy saving of centralized air-conditioning systems in subtropical Hong Kong. Applied Thermal Engineering. 2010;30:1659-65.

[7] Guo Y, Zhang G, Zhou J, Wu J, Shen W. A techno-economic comparison of a direct expansion ground-source and a secondary loop ground-coupled heat pump system for cooling in a residential building. Applied Thermal Engineering. 2012;35:29-39.

[8] Dygert RK, Dang TQ. Mitigation of cross-contamination in an aircraft cabin via localized exhaust. Building and Environment. 2010;45:2015-26.

[9] Dygert RK, Dang TQ. Experimental validation of local exhaust strategies for improved IAQ in aircraft cabins. Building and Environment. 2012;47:76-88.

[10] Melikov AK, Bolashikov ZD, Brand M. Experimental investigation of performance of a novel ventilation method for hospital patient rooms. 21st Congress of International Federation of Hospital Engineering (IFHE)2010.

[11] Zítek P, Vyhlídal T, Simeunović G, Nováková L, Čížek J. Novel personalized and humidified air supply for airliner passengers. Building and Environment. 2010;45:2345-53.

[12] Melikov A, Bolashikov ZD, Georgiev E. Novel ventilation strategy for reducing the risk of airborne cross infection in hospital rooms. Proceedings of Indoor Air 2011. 2011:1037.

[13] Qian H, Li Y, Nielsen PV, Hyldgaard CE. Dispersion of exhalation pollutants in a two-bed hospital ward with a downward ventilation system. Building and Environment. 2008;43:344-54.

[14] Cheong K, Phua S. Development of ventilation design strategy for effective removal of pollutant in the isolation room of a hospital. Building and Environment. 2006;41:1161-70.

[15] Nielsen PV, Li Y, Buus M, Winther FV. Risk of cross-infection in a hospital ward with downward ventilation. Building and Environment. 2010;45:2008-14.

[16] Yang J, Sekhar C, Wai DCK, Raphael B. Computational fluid dynamics study and evaluation of different personalized exhaust devices. HVAC&R Research. 2013;19:934-46.

[17] Bolashikov Z, Melikov A, Krenek M. Control of the free convective flow around the human body for enhanced inhaled air quality: Application to a seat-incorporated personalized ventilation unit. HVAC&R Research. 2010;16:161-88.

[18] Junjing Y, Sekhar C, Cheong D, Raphael B. Performance evaluation of an integrated Personalized Ventilation–Personalized Exhaust system in conjunction with two background ventilation systems. Building and Environment. 2014;78:103-10.

[19] Licina D, Melikov A, Pantelic J, Sekhar C, Tham KW. Human convection flow in spaces with and without ventilation: personal exposure to floor-released particles and cough-released droplets. Indoor air. 2015.

[20] Pereira M, Graudenz G, Tribess A, Morawska L. Determination of particle concentration in the breathing zone for four different types of office ventilation systems. Building and Environment. 2009;44:904-11.

[21] Ahmed AQ, Gao S. Thermal Comfort and Energy Saving Evaluation of a Combined System in an Office Room Using Displacement Ventilation. World Academy of Science, Engineering and Technology, International Journal of Mechanical, Aerospace, Industrial, Mechatronic and Manufacturing Engineering. 2015;9:1078-83.

[22] Ahmed AQ, Gao S, Kareem AK. A numerical study on the effects of exhaust locations on energy consumption and thermal environment in an office room served by displacement ventilation. Energy Conversion and Management. 2016;117:74-85.

[23] Hussain S, Oosthuizen PH. Numerical investigations of buoyancy-driven natural ventilation in a simple atrium building and its effect on the thermal comfort conditions. Applied Thermal Engineering. 2012;40:358-72.

[24] Cheng Y, Niu J, Liu X, Gao N. Experimental and numerical investigations on stratified air distribution systems with special configuration: Thermal comfort and energy saving. Energy and Buildings. 2013;64:154-61.

[25] Horikiri K, Yao Y, Yao J. Numerical study of unsteady airflow phenomena in a ventilated room. ICHMT DIGITAL LIBRARY ONLINE. 2012.

[26] Horikiri K, Yao Y, Yao J. Modelling conjugate flow and heat transfer in a ventilated room for indoor thermal comfort assessment. Building and Environment. 2014;77:135-47.
[27] Srebric J, Chen Q. Simplified numerical models for complex air supply diffusers. HVAC&R Research. 2002;8:277-94.
[28] Yuan X, Chen Q, Glicksman LR, Hu Y, Yang X. Measurements and computations of room airflow with displacement ventilation. Ashrae Transactions. 1999;105:340.
[29] Yakhot V, Orszag S, Thangam S, Gatski T, Speziale C. Development of turbulence models for shear flows by a double expansion technique. Physics of Fluids A: Fluid Dynamics (1989-1993). 1992;4:1510-20.
[30] Fluent A. 14.5, Theory Guide; ANSYS. Inc, Canonsburg, PA. 2012.
[31] Chandrasekhar S. Radiative heat transfer. Dover Publications, New York. 1960;11:11-2.
[32] Zhang Z, Chen Q. Comparison of the Eulerian and Lagrangian methods for predicting particle transport in enclosed spaces. Atmospheric Environment. 2007;41:5236-48.
[33] Nazaroff WW. Indoor particle dynamics. Indoor air. 2004;14:175-83.
[34] Zhao B, Zhang Y, Li X, Yang X, Huang D. Comparison of indoor aerosol particle concentration and deposition in different ventilated rooms by numerical method. Building and Environment. 2004;39:1-8.
[35] Li A, Ahmadi G. Dispersion and deposition of spherical particles from point sources in a turbulent channel flow. Aerosol Science and Technology. 1992;16:209-26.
[36] Saffman P. The lift on a small sphere in a slow shear flow. Journal of fluid mechanics. 1965;22:385-400.
[37] McLaughlin JB. Aerosol particle deposition in numerically simulated channel flow. Physics of Fluids A: Fluid Dynamics (1989-1993). 1989;1:1211-24.
[38] Nazaroff WW, Cass GR. Mathematical modeling of indoor aerosol dynamics. Environmental Science & Technology. 1989;23:157-66.

[39] Rizk M, Elghobashi S. The motion of a spherical particle suspended in a turbulent flow near a plane wall. Physics of Fluids (1958-1988). 1985;28:806-17.

[40] Wang M, Lin C-H, Chen Q. Advanced turbulence models for predicting particle transport in enclosed environments. Building and Environment. 2012;47:40-9.

[41] Romano F, Marocco L, Gustén J, Joppolo CM. Numerical and experimental analysis of airborne particles control in an operating theater. Building and Environment. 2015;89:369-79.

[42] Zhang Z, Chen Q. Experimental measurements and numerical simulations of particle transport and distribution in ventilated rooms. Atmospheric environment. 2006;40:3396-408.

[43] Hinds WC. Aerosol technology: properties, behavior, and measurement of airborne particles. New York, Wiley-Interscience, 1982 442 p. 1982;1.

[44] Xu Y, Yang X, Yang C, Srebric J. Contaminant dispersion with personal displacement ventilation, Part I: Base case study. Building and Environment. 2009;44:2121-8.

[45] Chen F, Simon C, Lai AC. Modeling particle distribution and deposition in indoor environments with a new drift–flux model. Atmospheric Environment. 2006;40:357-67.

[46] Fanger PO. Thermal comfort. Analysis and applications in environmental engineering. Thermal comfort Analysis and applications in environmental engineering. 1970.

[47] Horikiri K, Yao Y, Yao J. Numerical optimisation of thermal comfort improvement for indoor environment with occupants and furniture. Energy and Buildings. 2015;88:303-15.

[48] ASHRAE A. Standard 55-2004, Thermal Environmental Conditions for Human Occupancy, Atlanta: American Society of Heating, Refrigerating, and Air-conditioning Engineers. Inc, USA. 2004.

[49] Lian Z, Wang H. Experimental study of factors that affect thermal comfort in an upward-displacement air-conditioned room. HVAC&R Research. 2002;8:191-200.

[50] Zhang T, Chen QY. Novel air distribution systems for commercial aircraft cabins. Building and Environment. 2007;42:1675-84.

[51] Sadrizadeh S, Holmberg S. Effect of a portable ultra-clean exponential airflow unit on the particle distribution in an operating room. Particuology. 2015;18:170-8.